# Numerical Experiments on Consistent Horizontal and Vertical Resolution for Atmospheric Models and Observing Systems

MICHAEL S. FOX-RABINOVITZ*

*Laboratory for Atmospheres, NASA/Goddard Space Flight Center, Greenbelt, Maryland*

RICHARD S. LINDZEN

*Center for Meteorology and Physical Oceanography, Massachusetts Institute of Technology, Cambridge, Massachusetts*

(Manuscript received 30 September 1991, in final form 13 April 1992)

ABSTRACT

Simple numerical experiments are performed in order to determine the effects of inconsistent combinations of horizontal and vertical resolution in both atmospheric models and observing systems. In both cases, we find that inconsistent spatial resolution is associated with enhanced noise generation.

A rather fine horizontal resolution in a satellite-data observing system seems to be excessive when combined with the usually available relatively coarse vertical resolution. Using horizontal filters of different strengths, adjusted in such a way as to render the effective horizontal resolution more consistent with vertical resolution for the observing system, may result in improvement of the analysis accuracy. The increase of vertical resolution for a satellite-data observing system is, however, desirable. For the conventional-data observing system with better vertically resolved data, the results are different in that little or no horizontal filtering is needed to make spatial resolution more consistent for the system.

The obtained experimental estimates of consistent vertical and effective horizontal resolution are in a general agreement with consistent resolution estimates previously derived theoretically by the authors.

## 1. Introduction

Along with improvements of initial data quality, numerical schemes, diabatic parameterization methods, and availability of more powerful computer systems, the gradual increase of horizontal and vertical resolution was one of the most important and straightforward components of the substantial improvement, in terms of the increased accuracy and practical reliability, of NWP models and GCMs during the last two decades.

Some currently used operational forecast or experimental models have fine and very fine horizontal resolution of the order of a few to several tens of kilometers for hurricane and mesoscale models, 50–150 km for regional, and 60–300 km for global models and GCMs. At the same time, these models usually have a relatively limited number of levels in the vertical in the troposphere, and even poorer vertical resolution in the stratosphere. The vast majority of currently used NWP models and GCMs, even those with fine and very fine horizontal resolution, have no more than 6–19 levels for the whole tropospheric and lower stratospheric vertical domain of integration. Note that recently some leading modeling groups have been considering the possibility of increasing the model vertical resolution. An example is the new 31-level European Centre for Medium-Range Weather Forecasts (ECMWF) model (Simmons 1991). The same is true for current observing systems that have vertical resolution that is often even poorer than the aforementioned model resolution.

The discussion of consistent spatial resolution for numerical models and observing systems is presented in Lindzen and Fox-Rabinovitz (1989), hereafter referred to as LF. This paper contains some approximate estimates of consistent horizontal and vertical resolution for quasigeostrophic and gravity-wave processes. It is worth emphasizing that even according to some of the most moderate estimates, the vertical resolution needed for describing quasigeostrophic processes in middle latitudes should be increased (sometimes significantly) in order to be consistent with horizontal model resolution used by many models. As recently noted by Persson and Warner (1991), inconsistent resolution can be shown to produce spurious gravity waves. This is broadly consistent with the present finding of increased "noisiness."

There are three different types of spatial resolutions related to atmospheric models and observing systems, namely, physical, computational, and observational resolutions. The last may be defined, for example, as

* Universities Space Research Association.

*Corresponding author address:* Dr. Michael S. Fox-Rabinovitz, Laboratory for Atmospheres, NASA, Goddard Space Flight Center, Code 910.3, Greenbelt, MD 20771.

a mean distance in the horizontal and in the vertical between observation locations. Such an observational-resolution measure may be specified for particular regions.

Computational requirements on spatial model resolution allow us to keep a truncation error, or an accuracy of approximation within some reasonable range. It should guarantee, for example, that all physical scales resolved by a model are adequately represented by an appropriate number of grid points, or in other words, realistically described by a discretized system with a guaranteed approximation accuracy. The computational resolution usually imposes the strongest requirements on the number of grid points needed to represent the considered scales adequately.

The physically consistent resolution requirements that will be discussed, have to be derived from the basic properties of the atmospheric processes, and have to reflect, or correspond, to their nature. The requirements of this kind on physically consistent horizontal and vertical resolution for large-scale atmospheric models and observing systems are based on consideration of quasigeostrophic flows, tropical, and gravity-wave processes according to LF. Note that the vertical-resolution requirements for the tropical domain and especially for gravity-wave processes appear to be much more demanding than those for quasigeostrophic flows. Notice also that the problem of optical vertical discretization for atmospheric models has been discussed by Baer and Ji (1989).

According to LF, for quasigeostrophic flows the consistent combination of horizontal ($\Delta L$) and vertical ($\Delta Z$) scales is derived from the well-known relationship

$$\Delta L = \frac{N}{f_0} \Delta Z, \tag{1}$$

where $f_0$ is the characteristic Coriolis parameter and $N$ is the Brunt–Väisälä frequency.

For a regular spherical coordinate grid, Table 1 (taken from LF) shows the approximately consistent horizontal- and vertical-resolution combinations for different latitudes.

It is worth mentioning that spatial-resolution inconsistency is usually screened in atmospheric models by a rather strong spatial and/or temporal computational filtering applied to get rid of undesirable noise and/or to meet computational stability requirements. On the other hand, the substantial irregularity of conventional-data distribution and the use of satellite data swaths, usually only over the oceans for specific observation-time windows, make it difficult to trace the spatial- and temporal-resolution inconsistency for global observing systems.

TABLE 1. Consistent vertical- and horizontal-resolution combinations.

| Horizontal resolution (deg) | Vertical resolution (km) | | |
|---|---|---|---|
| | Local 60° | Local 45° | Local 22.5° |
| 1 | 0.34 | 0.39 | 0.28 |
| 2 | 0.68 | 0.78 | 0.55 |
| 4 | 1.35 | 1.55 | 1.10 |
| 8 | 2.70 | 3.10 | 2.19 |
| 16 | 5.40 | 6.20 | 4.40 |

This note is devoted to approximate experimental estimates of physically consistent horizontal and vertical resolution for atmospheric models and observing systems. When designing numerical experiments in order to show, directly and clearly, the effects of different model or observing system horizontal- and vertical-resolution combinations, we find that it is often difficult to separate the impact due exclusively to physical consistency of horizontal and vertical resolution from other virtually inevitable and mostly computational components of the performed calculations. In order to address the issue as straightforwardly as possible, we have taken some highly simplified approaches, and the obtained results should be considered as only approximate estimates of a spatial-inconsistency signal we are trying to detect.

The results of numerical experiments with models having different horizontal and vertical resolutions are presented in section 2. The experiments with observing systems are described in section 3. Section 4 contains some concluding remarks. The primitive equation (PE) baroclinic atmospheric model and analytical initial conditions are briefly described in the Appendix.

## 2. Results of numerical experiments with atmospheric models

The hypothesis we wish to verify is as follows: If the numerical approximation of model equations is accurate enough, and appropriate physically consistent requirements for vertical and horizontal resolution are fulfilled, the model should generate less noise than when such requirements are violated. If this hypothesis is correct, then estimated model lifetime (by which we mean the time needed for a model to break down) is a reasonable measure of model noise growth for different horizontal- and vertical-resolution combinations. We would like to know how model lifetime depends on resolution. The channel model and analytical initial conditions used for the experiments are briefly described in the Appendix.

Let us consider the results of numerical experiments with different model spatial-resolution versions in terms of model lifetimes. The different combinations of model horizontal and vertical resolutions are tested in the range of 50–400 km in the horizontal, and from 0.375 to 3.0 km in the vertical.

Simple analytical initial fields of a wave type superimposed on the constant zonal flow are used. Random noise in the range of ±20 m and ±2 m $s^{-1}$ has been

superimposed on initial height and wind fields, respectively. Such an initial noise imitates an imbalance of initial conditions, and makes the model breakdown periods relatively shorter.

It is evident that the model will generate all scales (even those that are not present in initial conditions) eventually, and error growth in time depends on many different model properties and parameters quite apart from those pertaining to the numerical scheme used and its truncation errors. We have, however, attempted to constrain our experiments to show primarily the sensitivity of model-generated noise to different combinations of horizontal and vertical resolution.

The model integrations continued until the tendencies of potential temperature exceeded 300 K $h^{-1}$, which we took to unambiguously indicate a model breakdown.

The results of the numerical experiments with the channel model are summarized in Table 2, where the lifetimes for different combinations of horizontal and vertical resolution are shown.

According to Table 2, the maximum lifetime period is obtained for the coarsest spatial-resolution model version ($\Delta Z$ = 3 km, $\Delta S$ = 400 km). Starting from that model version and increasing only horizontal or only vertical model resolution results in a decrease of lifetime periods (see the first line and the first column of Table 2).

On the other hand, there are some specific combinations of horizontal and vertical model resolution, which lie on or near the diagonal of Table 2, which result in a relative increase of lifetimes. These particular combinations are as follows: $\Delta z$ = 3 km and $\Delta S$ = 400 km; $\Delta z$ = 1.5 km and $\Delta S$ = 200 km; $\Delta z$ = 0.75 km and $\Delta S$ = 200 km; $\Delta z$ = 0.375 km and $\Delta S$ = 50 km. These optimal combinations correspond approximately to estimates of consistent resolution in LF (see Table 1). Other combinations generate more noise as manifested by reduced model lifetimes.

The aforementioned runs were repeated with a model modified by the introduction of very weak horizontal filtering in the form of a very high (32d) order Shapiro filter (Shapiro 1970). This filter filters out only scales smaller than approximately 2–2.5$\Delta S$. Moreover, the filtering largely eliminates the initially superimposed random noise. Therefore, the model lifetimes are noticeably extended. Similarly, the effective horizontal resolution is decreased by the filter.

TABLE 2. Model-lifetime estimates (days) for different combinations of horizontal and vertical resolution.

| Vertical resolution $\Delta Z$ (km) | Horizontal resolution $\Delta S$ (km) | | | |
|---|---|---|---|---|
| | 400 | 200 | 100 | 50 |
| 3.0 | 17.0 | 11.5 | 8.5 | 6.5 |
| 1.5 | 9.5 | 12.5 | 8.5 | 7.5 |
| 0.75 | 7.0 | 15.0 | 9.5 | 10.5 |
| 0.375 | 6.0 | 8.5 | 8.5 | 13.5 |

TABLE 3. Model-lifetime estimates (days) for different combinations of horizontal and vertical resolution, when applying very high (32d) order Shapiro filter [which filters out approximately (2–2.5)$\Delta S$ scales].

| Vertical resolution $\Delta Z$ (km) | Horizontal resolution $\Delta S$ (km) | | | |
|---|---|---|---|---|
| | 400 (×2 = 800) | 200 (×2 = 400) | 100 (×2 = 200) | 50 (×2 = 100) |
| 3.0 | 29.0 | 24.5 | 15.5 | 11.5 |
| 1.5 | 13.5 | 19.0 | 18.0 | 9.5 |
| 0.75 | 8.0 | 16.5 | 13.0 | 12.0 |
| 0.375 | 7.5 | 9.5 | 12.5 | 15.5 |

Note: The approximate effective resolution after filtering was applied is shown in the parentheses, where the factor of 2 corresponds to filtering scales smaller than 2$\Delta S$ that is an effective horizontal model resolution for the experiment.

Nonetheless, model lifetimes presented in Table 3 are qualitatively similar to those of Table 2 in the sense that the consistent, or optimal, combinations of horizontal and vertical resolution lie on or near the diagonal of the table. Optimal resolution combinations are $\Delta Z$ = 3 km and $\Delta S$ = 400–800 km; $\Delta Z$ = 1.5 km and $\Delta S$ = 200–400 km; $\Delta Z$ = 0.75 km and $\Delta S$ = 200–400 km; and $\Delta Z$ = 0.375 km and $\Delta S$ = 100 km. These optimal, or consistent, combinations also correspond to theoretical estimates of Table 1.

The numerical experiments described previously were performed with a specific channel model and analytical initial conditions. To see to what degree the conclusions derived are applicable to other models and initial data, we have looked at results obtained from runs with the adiabatic and diabatic versions of the fourth-order Goddard Laboratory for Atmospheres (GLA) GCM (Kalnay et al. 1983; Fox-Rabinovitz et al. 1991) with no filters applied and with corresponding, small time steps to avoid instability in polar domains. The real-data initial conditions used are valid at 0000 UTC 1 February 1979.

The model integration for each case continued until the sea level pressure departed from the limits of 1000 mb ± 300 mb; clearly, the model results were no longer physically realistic. Therefore, reaching these limits is considered to be a measure of model lifetimes for these cases. Notice, however, that the model integration could be formally continued. Note also that resolution combinations used are limited by model versions available.

The results of these adiabatic and diabatic model runs are presented in Table 4. Because we are using the global model (with the tropics included) and real data as initial conditions with all resolvable scales included, not applying any filters, using a higher fourth-order numerical scheme, and imposing more restrictive limits for surface pressures pointed out earlier, the model-lifetime estimates of Table 4 are substantially shorter than those of Tables 2 and 3. The results obtained with the adiabatic version of this model, how-

ever, also show that for the 4° × 5° horizontal resolution and the 2.2-km vertical resolution the model-lifetime estimate is the largest among all combinations considered for the adiabatic model, and the increase of the adiabatic model vertical resolution to 1.2 or 0.6 km leads to a substantial decrease of estimated model lifetime. This is true also for an increase of the horizontal adiabatic model resolution to 2° × 2.5°. At the same time, the increase of vertical adiabatic model resolution to 1.2 km for 2° × 2.5° horizontal resolution results in longer model lifetime, whereas the further increase of adiabatic model vertical resolution to 0.6 km for 2° × 2.5° horizontal resolution leads to a decrease of model survival time. Therefore, for the case of the adiabatic model, only two among all considered combinations of horizontal and vertical resolution, namely, 4° × 5°, 2.2 km, and 2° × 2.5°, 1.2 km, seem to be consistent (see Table 4). These results also correspond to the consistency requirements of LF.

We realize that the complete diabatic GCM, which includes besides dynamics the variety of parameterized physical processes (such as moist processes, turbulence, cloud–radiation interaction, and orographic effects), may impose additional requirements on consistent resolution combinations. Such a more complicated case does deserve a further detailed consideration, but it goes well beyond the goal of this qualitative study; however, we have performed experiments similar to those of the adiabatic model with the full diabatic GLA GCM, the results of which with available versions of the model are also presented in Table 4.

Note that on one hand, the full diabatic model may need finer vertical resolution to resolve, for example, moist processes, but on the other hand, the model turbulence works as a strong physical dumping mechanism controlling noise development that does not take place for the adiabatic model. For 4° × 5° horizontal-resolution versions of the diabatic model, the increase of vertical resolution from 2.2 to 1.2 km results in doubling the model lifetime, whereas the further increase of vertical resolution to 0.6 km leads to the significant decrease of the model lifetime. Therefore, the optimal, or consistent, spatial resolution for these diabatic model runs is 4° × 5°, 1.2 km. For 2° × 2.5° horizontal-resolution versions of the diabatic model, the increase of vertical resolution results in the increase of model lifetimes. The most consistent combination of horizontal and vertical resolution for the diabatic model among three considered cases is 2° × 2.5°, 0.6 km. Therefore, the tentative conclusion from the experiments with the diabatic model is that finer vertical resolution is needed than for the adiabatic model with the same horizontal resolution.

TABLE 4. Breaking-down periods (days) for the adiabatic and diabatic versions of the fourth-order GLA GCM when no filters are applied.

| Vertical resolution $\Delta Z$ (km) | Horizontal resolution, $\Delta S$ (deg) | | | |
|---|---|---|---|---|
| | 4 × 5 | | 2 × 2.5 | |
| | Adiabatic | Diabatic | Adiabatic | Diabatic |
| 2.2 | 3.0 | 2.5 | 2.0 | 1.0 |
| 1.2 | 2.0 | 5.0 | 2.5 | 1.5 |
| 0.6 | 0.6 | 2.0 | 1.0 | 2.5 |

The main conclusion of the experiments performed with both models is that when choosing or changing model spatial resolution, the approximate estimates shown in LF may provide some guidance for achieving physically consistent combinations of horizontal and vertical model resolution.

## 3. Numerical experiments with observing systems

Another type of numerical experiment, concerning the problem of consistent horizontal and vertical resolution, has been performed for two observation networks, namely, for the satellite-data and for conventional-data observing systems. Note that the satellite data is relatively poorly resolved in the vertical and much better resolved in the horizontal compared to conventional data. Therefore, we may expect that these two observing systems might reveal spatial-resolution inconsistency in different ways.

The new, substantially revised version of the GLA four-dimensional (4D) data-assimilation procedure of an intermittent type uses the optimum-interpolation (OI) objective analysis technique (Susskind and Pfaendtner 1989). The data-assimilation system was run for 10 days prior to the final analysis time, which, therefore, included 40 consecutive analysis and first-guess (or 6-h forecast) calculations. The forecast model used within the data-assimilation system is the 17-layer GLA GCM (Fox-Rabinovitz et al. 1991). The data used for the 4D data-assimilation experiments and analysis results are available at all 14 mandatory levels from 1000 to 20 mb. The data within satellite swaths are available with rather fine (approximately 100-km) horizontal resolution. The analysis system was run twice with 4° × 5° and 2° × 2.5° horizontal resolution to verify robustness of obtained results. For simplicity, these resolutions will be hereafter referred to as 4° and 2° horizontal resolutions, respectively.

The design of the experiments to verify the spatial-resolution consistency for the systems is as follows: For imitating different combinations of effective horizontal resolution with the given vertical resolution for both systems, horizontal filtering is used as a tool for changing effective horizontal resolution. Spherical harmonic filters (Swarztrauber 1979) of different strengths have been applied to analysis fields. Namely, the smaller scales have been sequentially filtered out by applications of filters with different truncations (or spectral cutoffs) corresponding to a wide range from 2° to 32°.

The unfiltered, as well as all filtered, analysis fields for both runs with 4° and 2° horizontal resolution have been verified against all available conventional data as

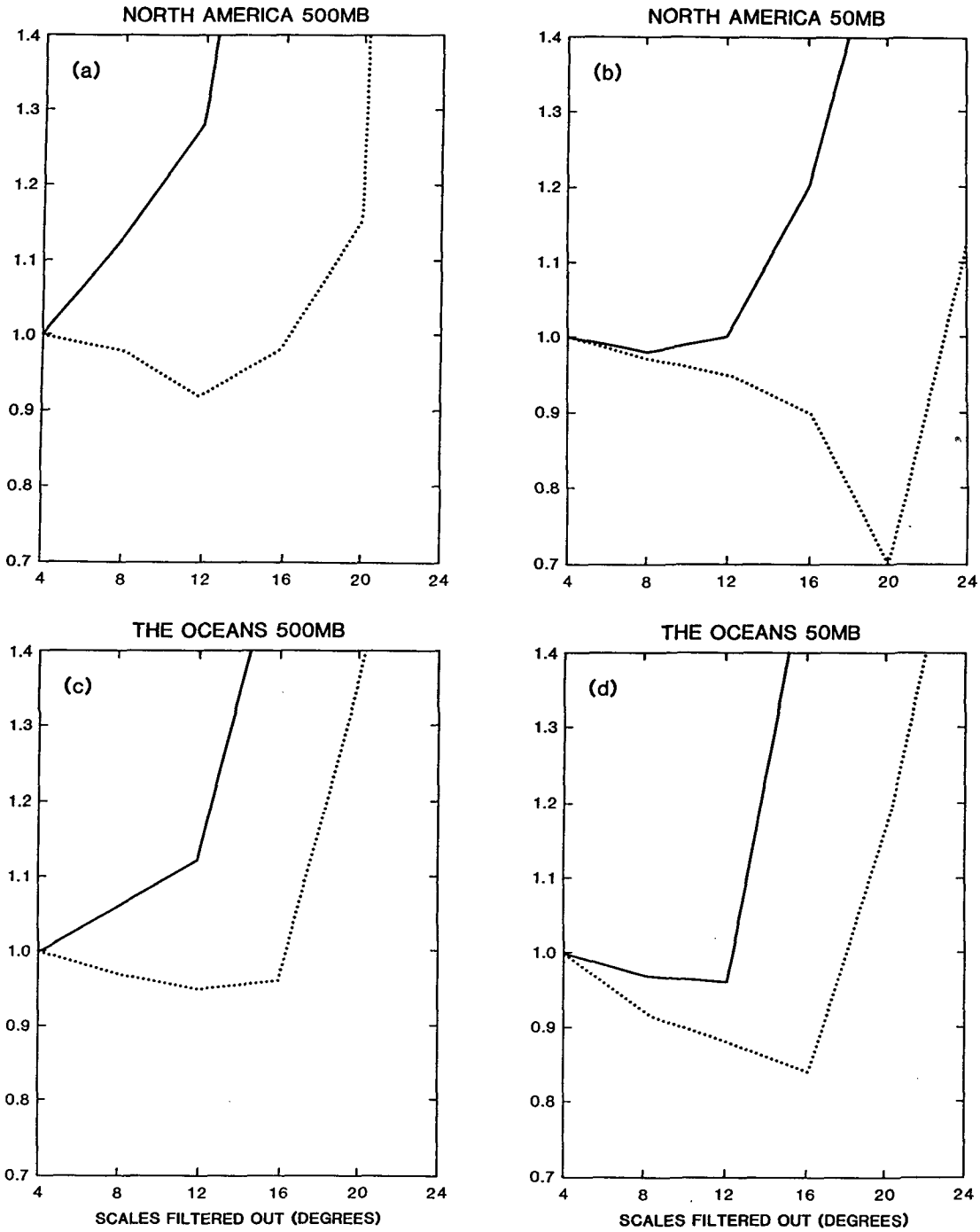


FIG. 1. Relative rms height-analysis errors (normalized by the corresponding rms error for unfiltered analysis fields valid at 0000 UTC 10 February 1979) as functions of effective horizontal resolution (obtained by an application of different strength filters) for the North American and the ocean regions and for 500- and 50-mb levels. The solid line is for the conventional-data analysis, and the dashed line is for the satellite-data analysis. The analyses for the case are calculated with 4° × 5° horizontal resolution.

the most reliable information, and rms differences, or errors, are calculated at observation locations over each continent and over the oceans.

It is assumed that the consistent combination of a given observational vertical resolution and an adjusted (through different strength filtering) effective horizontal resolution would manifest itself in decreasing or at least not substantially increasing rms analysis errors, compared to those of unfiltered fields.

In other words, the consistent, or optimal, combi-

nation of vertical and horizontal resolution is associated with a minimum of the rms error. This minimum may sometimes be rather flat, and then the consistent combinations correspond to some range of effective horizontal resolutions rather than to a particular one.

Figure 1 presents some examples of the dependence of rms analysis errors on filtering strength (or equivalently on effective horizontal resolution) for both observing systems (for the run with 4° horizontal resolution). The rms errors are normalized by those of corresponding, unfiltered analysis fields. The response to filtering is different for the two observing systems. For example, for conventional-data analysis over such a rich data region as North America, no filtering is usually needed in the troposphere (Fig. 1a), whereas for satellite-data analysis for the region, filtering the scales smaller than 12° results in decreasing the rms errors. Therefore, for this case, the effective horizontal resolution for conventional data is 4° (unfiltered fields). For satellite data, it is 12° because rms error is minimal for this effective horizontal resolution, but it grows significantly when stronger filters are applied.

The results of all experiments we performed are summarized in Table 5, where for given vertical observational resolutions of satellite and conventional networks, the consistent effective horizontal resolutions are presented for two thick layers (from 100 to 20 mb, and from 1000 to 150 mb), and for different regions (North America, Eurasia, and the oceans). Recall that for unfiltered fields, the horizontal resolutions are 4° or 2° for the two system runs performed.

The approximate observational vertical-resolution estimates for satellite data of Table 5 have been derived from Susskind and Reuter (1985). According to these estimates, the vertical resolution is approximately 2 km in the lower troposphere, and 4 km in the upper troposphere and lower stratosphere (below 100 mb). In the rest of the stratosphere, the vertical resolution of satellite data is markedly larger than 4 km.

The radiosonde data has finer vertical resolution of approximately 1.5 km in the lower troposphere, and 2 km in the upper troposphere and lower stratosphere. Above 100 mb, the vertical resolution for the data is in the range of 2 to 3.5 km, and coarser above. In general, the vertical resolution for the satellite data network is noticeably coarser than that of conventional data, especially in the stratosphere.

The corresponding estimates of effective horizontal resolutions that are consistent with a given vertical resolution for the two observing systems differ significantly. For the lower layer from 1000 to 150 mb for all regions, the combinations of the 2° effective horizontal resolution for lower tropospheric levels and 4° for other levels of the layer and the 1.5–2-km vertical resolution appeared to be optimal, or consistent, for the conventional-data analysis. For these cases, the unfiltered 2° or 4° analysis fields have minimal rms errors (Table 5).

For satellite-data analyses for the lower layer with 2–4-km vertical resolution, the consistent effective horizontal resolution is coarser than that of conventional data, and varies for different regions in the range of 8°–16°.

Qualitatively similar results have been obtained for both observing systems for the upper layer extending from 100 to 20 mb. Namely, for conventional data with 2–3.5-km vertical resolution, the consistent effective horizontal resolution varies from 4° to 12° for different regions, which is coarser than for the lower layer. This reflects the relative smoothness of analyses for upper levels due to characteristic scales of the fields and to a gradual decrease with height of data availability and quality.

For satellite data with definitely more than 4-km vertical resolution for the layer, the consistent effective horizontal resolution varies from 12° to 24° for different regions, which is substantially coarser than that of conventional data.

Because of lack of vertical resolution for satellite data (especially in the upper layer), it may not be necessary or useful to keep increasing the already high horizontal resolution, until finer vertical resolution for the data is available. Therefore, the increase of vertical resolution for satellite data seems to be desirable to match a fine horizontal resolution of the data.

The results described previously (Table 5) are fairly close for two analysis runs with different horizontal resolutions, 4° and 2°. The only difference is that over the North American and Eurasian continents with dense conventional networks, the unfiltered conventional-data analyses calculated with the 2° horizontal

TABLE 5. Consistent or optimal combinations of a given observational vertical resolution and an effective (or adjusted through filtering) horizontal resolution for different layers and regions for both satellite and conventional observing systems.

| | Approximate observational vertical resolution (km) | | Effective horizontal resolution (deg) | |
|---|---|---|---|---|
| Layer (mb) | Satellite data | Conventional data | Satellite data | Conventional data |
| | | North America | | |
| 100–20 | >4.0 | 2.0–3.5 | 16–24 | 4–12 |
| 1000–150 | 2.0–4.0 | 1.5–2.0 | 12 | 2*–4 |
| | | Eurasia | | |
| 100–20 | >4.0 | 2.0–3.5 | 12–16 | 4–8 |
| 1000–150 | 2.0–4.0 | 1.5–2.0 | 8–12 | 2*–4 |
| | | Oceans | | |
| 100–20 | >4.0 | 2.0–3.5 | 12–16 | 4–12 |
| 1000–150 | 2.0–4.0 | 1.5–2.0 | 12–16 | 4 |

* For lower-tropospheric levels (1000, 850, and sometimes 700 mb).

resolution seem to be more accurate for the lower-tropospheric levels, or for 1000-, 850-, and sometimes 700-mb levels.

In practice, both conventional and satellite data are used. According to obtained results, it may make sense to implement a two-stage analysis procedure: namely, to calculate, for example, first an analysis using only satellite data, and then smooth it in the horizontal and proceed with calculating an analysis with only conventional data using the smoothed satellite-data analysis as a first guess.

The obtained estimates of consistent vertical and horizontal resolution for both observing systems are again in approximate agreement with the theoretical estimates of LF (see Table 1).

## 4. Conclusions

This paper has examined the consequences of inconsistent horizontal and vertical resolution in both atmospheric models and observing systems by means of some highly simplified experiments.

An adiabatic PE baroclinic atmospheric model with analytical initial conditions and cyclic boundary conditions (a channel model) and the adiabatic and diabatic versions of the GLA GCM are used for the model experiments. Suitably defined model lifetimes are compared for different horizontal and vertical model resolution combinations under the assumption that noisier models will have shorter lifetimes. Our aim was to see whether consistent resolution helped minimize model noise. For numerical experiments with the channel model, the forecasts with disturbed initial conditions (where random noise was superimposed) were used for comparisons of different combinations of the spatial resolutions. Model lifetime, in these cases, referred essentially to the time it took a model run to "blow up." Such lifetimes are reasonable estimates of the forecast error developments in time that are associated primarily with model physical spatial resolution inconsistency.

The experiments with atmospheric models have shown that some consistent combinations of horizontal and vertical resolution exist for which lifetime-period estimates are relatively larger, or noise generated due to spatial resolution inconsistency is smaller (Table 4). These estimates also correspond approximately to those obtained in LF (Table 1).

Experiments were also performed in order to determine the implications of consistent resolution for observing systems. In these experiments, we compared satellite- and conventional-data networks. Objective analyses of heights and winds using either satellite data alone or conventional data alone were calculated, and then spherical harmonic filters of different strengths were applied in order to change effective horizontal resolution. All analysis experiments were run twice, with 4° and 2° horizontal resolution, to verify the robustness of obtained results.

It is suggested that the consistent combination of a given observational vertical resolution and an adjusted (through different strength filtering) effective horizontal resolution would result in decreasing, or at least not substantially increasing, rms analysis errors compared to those of unfiltered fields. Therefore, the consistent, or optimal, vertical and horizontal resolution is associated with a minimum of a rms error. The minimum may sometimes be rather flat, and then the consistent combinations correspond to some range of effective horizontal resolutions rather than to a particular one. In such cases, however, no evident advantage results from the finer resolutions.

The experiments with conventional and satellite data have resulted in substantially different consistent spatial-resolution combinations (Table 5). Namely, for satellite data with relatively poorer vertical resolution the consistent effective horizontal resolution is coarser than that of conventional data.

The experiments with the observing systems have shown that an excessive horizontal resolution in combination with a relatively poor vertical resolution may result in larger analysis rms errors compared to those of a network with more consistent spatial resolution. The increase of vertical resolution for satellite data to match a fine horizontal resolution of the data is desirable. The results are again in qualitative agreement with the estimates of LF (Table 1).

In brief, using consistent horizontal and vertical resolution for both atmospheric models and observing systems appears desirable for better representation of large-scale atmospheric phenomena and processes, and is certainly more economical.

*Acknowledgments.* The authors want to thank Mr. R. Govindaraju, Mr. M. Seablom, and Mr. D. Lamich for programming support, and Mrs. Q. Philpot for typing the manuscript. The research was supported by NASA Grant 578-41-25-20 at the Goddard Space Flight Center, and by NASA Grant NAGW 525 and National Science Foundation Grant ATM 8520354 at the Massachusetts Institute of Technology.

## APPENDIX

## The Experimental PE Model and Analytical Initial Conditions

### *a. A brief description of the channel model and numerical scheme*

For the numerical experiments in the text, the PE adiabatic baroclinic atmospheric model (with only surface friction included) in $x, y, p$ coordinate system, and with cyclic boundary conditions, and simple analytical initial data is used.

The calculation of analytical initial data for the numerical experiments is done following Fritsch et al. (1980), and is described below.

For the finite-difference approximation of the model equations, the horizontal, Arakawa C grid (Mesinger and Arakawa 1976; Arakawa and Lamb 1977), and a uniform vertical grid of Lorenz type (Lorenz 1960) was used. For the time integration, the economical explicit scheme (Brown and Compana 1978; Fox-Rabinovitz 1974) was applied.

No space filters are applied, but the time filter (Asselin 1972) is used to control the computational mode of the leapfrog scheme.

The time step $\Delta t$, when using the economical explicit scheme for the model version with the horizontal increment $\Delta s$ = 400 km, is 16 min, and for other model versions with finer horizontal resolution is correspondingly smaller according to the CFL criterion. The horizontal integration domain is a square with the sides equal to 4000 km. In the vertical a uniform grid in $\ln p$ was used for all vertical model resolution versions.

To be able to perform these rather time-consuming experiments with all model versions more efficiently, the split-explicit integration scheme (Gadd 1978) was applied in combination with the economical explicit scheme.

The application of the split-explicit scheme allows using time steps that are three times longer for the horizontal-advection subsystem. Finally, for the horizontal resolution with $\Delta s$ = 400 km, the time step for the adjustment subsystem is $\Delta t$ = 16 min, and for the advection subsystem $\Delta t$ = 48 min. For other horizontal-resolution model versions, the time steps are correspondingly smaller.

### b. *Calculation of analytical initial data*

Analytical initial conditions at pressure levels are calculated following Fritsch et al. (1980). The analytical data of a wave type are superimposed on a constant zonal flow. The analytical data calculation consists of the following steps: 1) calculation of analytical heights for the 1000-mb level using the mean height for the level estimated from real data; 2) computation of real potential temperatures from real-data geopotentials using the hydrostatic equation, and determining the real vertical mean temperature profile; 3) calculation of analytical temperature fields using the real mean temperature profile; 4) calculation of analytical geopotentials for all levels above 1000 mb from analytical potential temperatures by hydrostatic equation; and 5) calculation of analytical winds for all levels from analytical geopotentials using the geostrophic relationship.

## REFERENCES


Arakawa, A., and V. R. Lamb, 1977: Computational design of the basic dynamical processes of the UCLA general circulation model. *Methods of Computational Physics,* Vol. 17, Academic Press, 173–265.

Asselin, R., 1972: Frequency filter for time integrations. *Mon. Wea. Rev.*, **100,** 487–490.

Baer, F., and Ming Ji, 1989: Optimal vertical discretization for atmospheric models. *Mon. Wea. Rev.*, **117,** 391–406.

Brown, J. A., and K. Campana, 1978: An economical time-differencing system for numerical weather prediction. *Mon. Wea. Rev.*, **106,** 1125–1136.

Fox-Rabinovitz, M. A., 1974: On economical semi-implicit integration schemes for forecast equations. *Meteor. Gidrol.*, **11,** 11–19.

Fox-Rabinovitz, M. S., H. M. Helfand, A. Hou, L. L. Takacs, and A. Molod, 1991: Numerical experiments on forecasting, climate simulation and data assimilation with the new 17-layer GLA GCM. *Proc., Ninth NWP Conference,* Amer. Meteor. Soc., Denver, 506–509.

Fritsch, J. M., E. L. Magaziner, and C. F. Chappel, 1980: Analytical initialization for three-dimensional numerical models. *J. Appl. Meteor.*, **7,** 809–818.

Gadd, A. J., 1978: A split explicit integration scheme for numerical prediction. *Quart. J. Roy. Meteor. Soc.*, **104,** 569–582.

Kalnay, E., R. Balgovind, W. Chao, D. Edelman, J. Pfaendtner, L. Takacs, and K. Takano, 1983: Documentation of the GLAS fourth order GCM. NASA Tech. Memo., 86064, 294 pp.

Lindzen, R. S., and M. S. Fox-Rabinovitz, 1989: Consistent vertical and horizontal resolution. *Mon. Wea. Rev.*, **117,** 2575–2583.

Lorenz, E. N., 1960: Energy and numerical weather prediction. *Tellers,* **12,** 364–373.

Mesinger, F., and A. Arakawa, 1976: Numerical methods used in atmospheric models. WMO/ICSU Joint Organizing Committee, *GARP Publ. Series,* Vol. I, No. 17, 64 pp.

Persson, P. O. G., and T. T. Warner, 1991: Model generation of spurious gravity waves due to inconsistency of the vertical and horizontal resolution. *Mon. Wea. Rev.*, **119,** 917–935.

Shapiro, R., 1970: Smoothing, filtering and boundary effects. *Rev. Geophys. Space Phys.*, **8,** 359–387.

Simmons, A. J., 1991: Development of a high resolution, semi-Lagrangian version of the ECMWF forecast model. *Proc. Seminar on Numerical Methods in Atmospheric Models,* Reading, England, ECMWF, Vol. II, p. 281–324.

Susskind, J., and D. Reuter, 1985: Intercomparison of physical and statistical retrievals from simulated HIRS2 ana AMTS data. *Advances in Remote Sensing Retrieval Methods,* A. Deepak, H. E. Fleming, and M. T. Chahine, Eds., A. Deepak Publishing, 641–662.

——, and J. Pfaendtner, 1989: Impact of interactive physical retrievals on NWP. *Proc., Joint ECMWF/EUMETSAT Working Group on the Use of Satellite Data in Operational NWP,* Reading, England, ECMWF, 245–270.

Swarztrauber, P. N., 1979: On the spectral approximation of discrete scalar and vector functions on the sphere. *SIAM J. Num. Anal.*, **16,** 6–26.